World Academy of Science, Engineering and Technology
International Journal of Mechanical and Mechatronics Engineering
Vol:11, No:2, 2017

H-Infinity and RST Position Controllers of Rotary Traveling Wave Ultrasonic Motor

M. Brahim, I. Bahri, Y. Bernard

***Abstract*—**Traveling Wave Ultrasonic Motor (TWUM) is a compact, precise, and silent actuator generating high torque at low speed without gears. Moreover, the TWUM has a high holding torque without supply, which makes this motor as an attractive solution for holding position of robotic arms. However, their nonlinear dynamics, and the presence of load-dependent dead zones often limit their use. Those issues can be overcome in closed loop with effective and precise controllers. In this paper, robust H-infinity (H∞) and discrete time RST position controllers are presented. The H∞ controller is designed in continuous time with additional weighting filters to ensure the robustness in the case of uncertain motor model and external disturbances. Robust RST controller based on the pole placement method is also designed and compared to the H∞. Simulink model of TWUM is used to validate the stability and the robustness of the two proposed controllers.

***Keywords*—**Piezoelectric motors, position control, H∞, RST, stability criteria, robustness.

I. Introduction

TWUM generates motion when voltage is applied to piezoelectric ceramics in the frequency range exceeding people`s audible sound region (0-20 kHz). The vibration force of piezoelectric materials will generate flexural waves at the surface of the stator able to rotate the rotor pressed to it [1]. This silent motor is specially characterized by: its small sizes, high torque at low speed without gears, electromagnetic noise free operation, and high holding torque without supply. These characteristics make TWUM widely recommended for positioning applications at low speed such as: autofocus of camera, adjustment of lens mirrors for optical equipment, actuator within high magnetic field environment, and actuation of robot arms [2].

TWUM have also disadvantages that should be eliminated. The motor output characteristics are time-varying owing to change in motor driving conditions and temperature increasing. The presences of phase shift-speed dead zone due to torque load complicate the control of TWUM [3]. Therefore, to fully implement its potential performances, closed loop operation mode is often desired [11]. In order to validate the performance of TWUM in closed loop, precise and robust controller should be designed. The synthesis and implementation of such controller needs an accurate model that reflects the motor behavior.

Mouhanned Brahim, Imen Bahri, and Yves Bernard are with GeePs Group of Electrical Engineering – Paris UMR CNRS 8507, Centrale Supélec, Univ Paris-Sud, Sorbonne Universités, UPMC Univ Paris 06, 11 rue Joliot-Curie, Plateau de Moulon F-91192 Gif-sur-Yvette CEDEX (e-mail: mouhanned.brahim@geeps.centralesupelec.fr).

The position control task was widely reported in the literature. Fixed and variable gain PID is the most proposed controller [4], [5]. The Proportional–Integral–Derivative (PID) controller is simple and easy to be implemented but it is difficult to set the parameters while as long as the motor parameters are time varying. Neural Networks (NN) and Fuzzy Logic (FL) are reported in many research works [6]-[8]. The intelligent controllers give better accuracy. However, USM behavior and parameters variation yields to the growth of network's complexity for the NN controller which will increase the time execution and learning procedure [3]. The FL control is based on the knowledge of USM state and experimental data to make up the fuzzy interference rules. But, under certain conditions, the motor parameters are variable and the output motion can be outside the interference rules [3]. Adaptive methods determine control parameters on-line, compare output with reference model, and compensate displacement/speed error [9]. They give relatively advantageous results with USMs when they are designed based on accurate models.

In this paper, authors propose two robust position controllers to deal with high precision positioning system based on TWUM. The main challenge of those controllers is to overcome the nonlinear behavior due to the hysteresis, the motor parameters variation, and the effect of external disturbances. The proposed H∞ and RST controllers are designed, and simulated in closed loop with an accurate model of rotary TWUM from Shinsei Co. (USR60). The performances and robustness of the two controllers are then evaluated and compared.

II. Modeling of Rotary TWUM USR60

A. Operation Principle

The cutaway view of rotary TWUM (USR60) manufactured by Shinsei Co. is shown in Fig. 1. The stator is composed by piezoelectric materials to generate vibration and additional metal to amplify it. The rotor is made from bronze material and pressed against the stator. Two-phase shifted sinusoidal waves (VA, VB) with a frequency (f) close to the mechanical resonance frequency (f_r) supply two orthogonal modes of piezoelectric ceramic.

$$\begin{aligned} V_A &= V_{max} \sin(2\pi ft) \\ V_B &= V_{max} \sin(2\pi ft + \phi) \end{aligned} \quad (1)$$

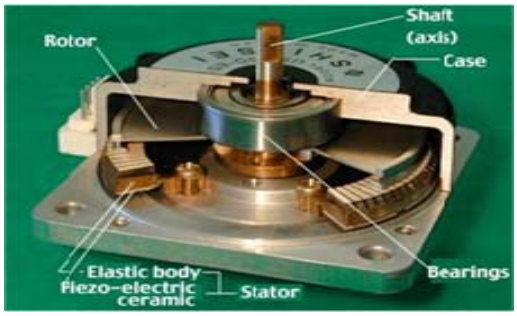

Fig. 1 Cutaway view of USR60 [2]

The shape of the ceramic will change and the vibration will be amplified by the stator metal [1]. Traveling wave is then generated on the stator surface and elliptical motion of wave will be created. The stator metal will touch the rotor only at each peak of a traveling wave. As response of the elliptical movement, the rotor will rotate in the opposite direction of the traveling wave propagation [12].

B. Modeling Approach

The detailed model of USR60 is presented in [10]. The model should reflect the variation of motor output characteristics as function of internal parameters (coupling factor, damping, stiffness, frictional forces…) and driving parameters (voltage amplitude, frequency, and phase shift). In the other side, this model will be easily controlled in the two rotation directions via driving voltages, frequency, or phase shift. When supplying the motor, two standing waves will be created at the stator. The standing waves spread equations can be written as:

$$\begin{aligned} M_{eff}\ddot{\xi}_1 + C_{S1}\dot{\xi}_1 + K_{s1}\xi_1 &= \eta V_A + F_{fs1} \\ M_{eff}\ddot{\xi}_2 + C_{S1}\dot{\xi}_2 + K_{s1}\xi_2 &= \eta V_B + F_{fs2} \end{aligned} \quad (2)$$

where: $\xi_{1.2}$ are the amplitudes of standing waves, Meff, $Cs_{1,2}$, $Ks_{1,2}$, and η are respectively the effective mass, damping, spring coefficient, and piezoelectric force factor of the stator. $F_{fs1,\,2}$ are the feedback forces generated by the stator.

The amplitude of resulting Traveling Wave (TW) can be then calculated as:

$$\xi_{max} = \sqrt{\xi_1^{\,2} + \xi_2^{\,2}} \quad (3)$$

The angular velocity of the rotor Ω_{rotor} can be then deduced:

$$J_r \frac{d\Omega_{rotor}}{dt} = T_{usm} - T_{load} \quad (4)$$

where J_r is the inertia of the rotor, T_{load}, T_{USM} are the load and motor torques.

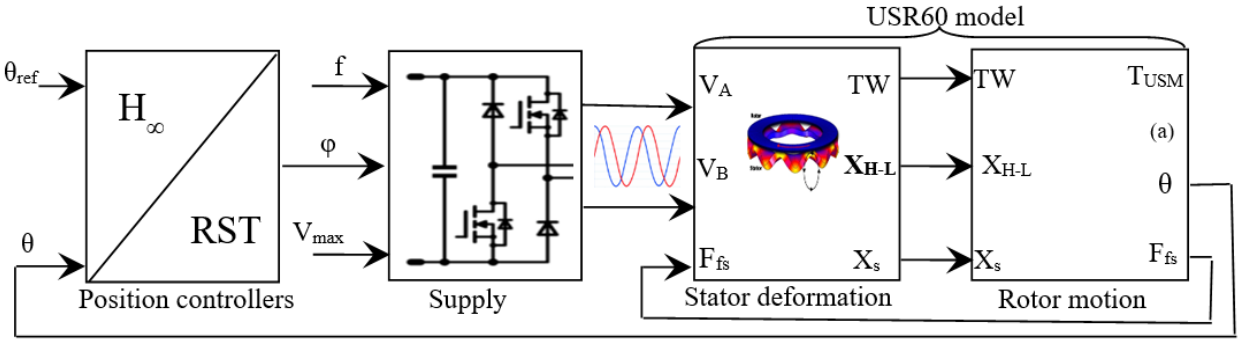

Fig. 2 Block diagram of the simulated closed loop system

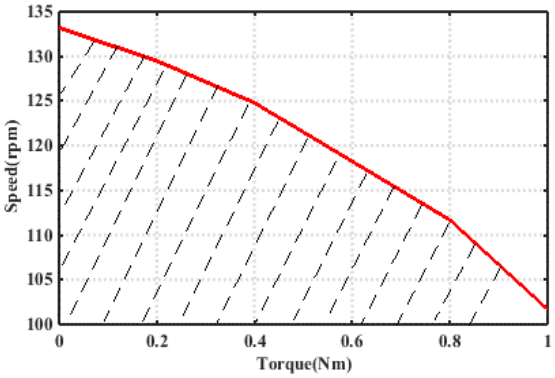

Fig. 3 Speed-Load characteristic

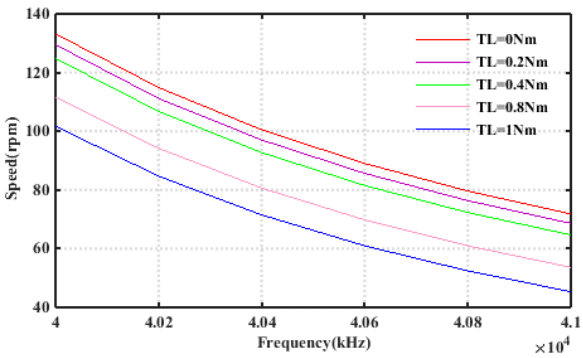

Fig. 4 Effect of load torque on the motor velocity

The USR60 model is implemented in MATLAB/Simulink environment to validate its performance before applying the closed loop position controller. The output characteristics of USR60 model are verified. The speed-torque characteristic is shown in Fig. 3 at the driving frequency of 40 kHz (mechanical resonance frequency), while the voltage amplitude is equal to 130 Vrms and the phase shift equal to 90°. The dashed zone in Fig. 3 corresponds to the operation zone of USR60. The effect of additional load torque at the angular velocity in the frequency range above the resonance (40-41 kHz) was also shown in Fig. 4. The variation of the rotational speed as function of the voltage amplitude (Vrms) and phase shift (φ) is illustrated in Fig. 5. From the last figure, it is clear that the speed-voltage amplitude characteristic represents quasi-linear behavior but the speed change slowly when voltage vary between 90 and 130 Vrms. Thus, using the voltage amplitude as control parameter will limit the motor motion and for only one rotation direction. The voltage phase shift (φ) gives the possibility to change the rotation direction with precision but represents a non-linearity around zero-phases especially when load torque is added.

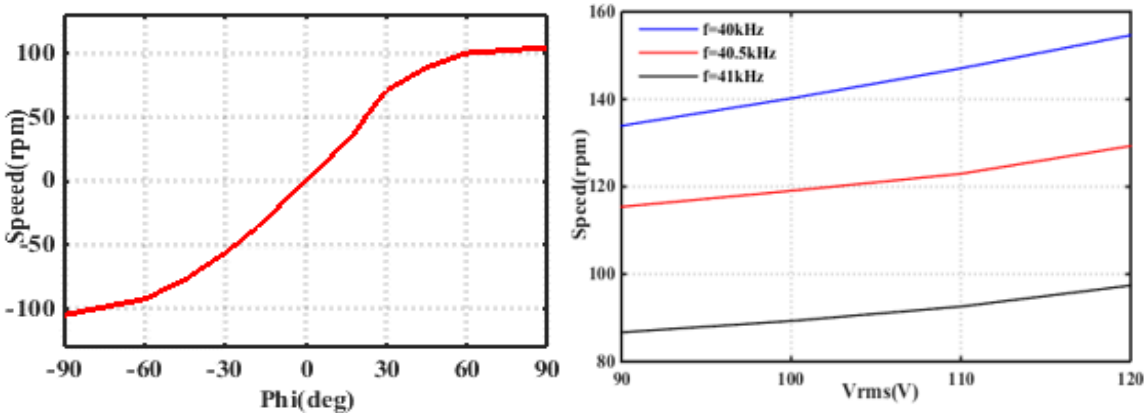

(a) (b)

Fig. 5 Motor speed as function of: (a) Phase shift (φ), Voltage amplitude (Vrms)

III. Synthesis of H∞ TWUM Position Controller

In this section, the synthesis approach of robust H∞ position controller is detailed. It should be mentioned before, that the voltage phase difference (φ) was chosen as position controller parameter based on simulation results and the intended application of the motor (robotic applications with high precision levels and bidirectional operation mode). The transfer function between the position (θ) and φ is given by [13]:

$$\frac{\theta(s)}{\varphi(s)} = \frac{k_m}{s(1+\tau s)} \tag{5}$$

where k_m=10.25 is the gain, and τ=3.5 ms is the time constant.

The dynamic behavior of the ultrasonic motor will automatically change as function of driving parameters and operation conditions (temperature, load, etc.). As a result, the dynamic model parameters (5) will change [12]. We count on the designed robust controllers to overcome the uncertain model problem. The synoptic of proposed system including motor model, supply, and position controllers is shown in Fig. 2. It is well known from robust control theory that any block diagram can be rearranged into the standard form shown in Fig. 6. The transfer matrix of generalized system can be written as [15]:

$$\begin{pmatrix} E(s) \\ Y(s) \end{pmatrix} = P(s) \begin{pmatrix} W(s) \\ U(s) \end{pmatrix} = \begin{pmatrix} P_{ew}(s) P_{eu}(s) \\ P_{yw}(s) P_{yu}(s) \end{pmatrix} \begin{pmatrix} W(s) \\ U(s) \end{pmatrix} \tag{6}$$

The lower Linear Fraction Transformation (LFT) between w and e is then:

$$E(s) = F_l(P(s), K(s)) W(s) \tag{7}$$

$$F_l(P(s), K(s)) = P_{ew}(s) + P_{eu}(s) K(s) (I - P_{yu}(s) K(s))^{-1} P_{yw}(s) \tag{8}$$

The synthesis of H∞ controller consists of finding a state feedback controller K(s) that should in any case internally stabilize the closed loop system, and guaranteeing that the H∞ norm satisfies the following inequality [15]:

$$\left\| F_l(P(s), K(s)) \right\|_\infty \prec \gamma \tag{9}$$

There are several resolution methods for the standard H_∞ problem. Riccati equation method is still the most used [15], and is applied in this work to resolve the problem. In the block diagram of the closed loop system (Fig. 7 (a)), the motor model is represented by G(s), K(s) is the controller, b is an additional perturbation, r and y are respectively the reference and measured position. The transfer matrix of this system is:

$$\begin{pmatrix}\varepsilon\\ u\end{pmatrix}=\begin{pmatrix}K & SG\\ KS & KSG\end{pmatrix}\begin{pmatrix}r\\ b\end{pmatrix};\ S=\frac{1}{(1+KG)} \tag{10}$$

where S is the sensitivity function and it is the transfer function between the reference signal r and the tracking error ε. The controller K(s) must satisfy the following inequality:

$$\left\|\begin{matrix}K & SG\\ KS & KSG\end{matrix}\right\|_{\infty}\prec\gamma \tag{11}$$

To satisfy the inequality (11) and to improve the robustness of the controller, supplementary degree of freedom should be added to the system [16]. Therefore, weighting filters (W_i) are widely introduced [14] as shown in Fig. 7 (b). The transfer matrix will be then:

$$\begin{pmatrix}E_1\\ E_2\end{pmatrix}=\begin{pmatrix}W_1S & W_1SGW_3\\ W_2KS & W_2KSGW_3\end{pmatrix}\begin{pmatrix}R\\ D\end{pmatrix} \tag{12}$$

The controller K(s) will satisfy now the following inequality:

$$\left\|\begin{matrix}W_1S & W_1SGW_3\\ W_2KS & W_2KSGW_3\end{matrix}\right\|_{\infty}\prec\gamma \tag{13}$$

The advantage of using the topology shown in Fig. 7 (b) instead of Fig. 7 (a) is that the system response frequency will be fixed by the filter behaviors.

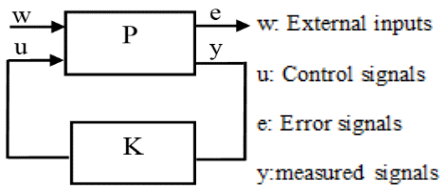

Fig. 6 Standard controlled system configuration

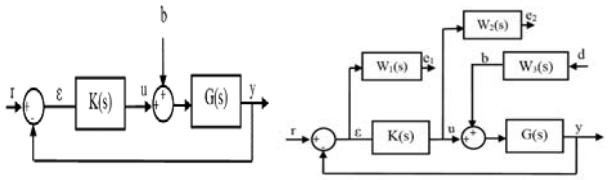

(a) (b)

Fig. 7 (a) Closed loop system configuration, (b) with weighting filters

The desired performances of the closed loop system as the robustness criteria will then be fixed via the filter parameters depending on the frequency operation range. For the USR60 system plant, the closed loop performances are fixed as:

- Time response: <10 ms
- Stability margin: ΔG>10 dB, Δφ>45
- Static error: < 0.1%

1) Choice of W_1: The transfer $1/W_1$ should have a low gain at low frequency to ameliorate the controller precision while the filter cut off frequency can be interpreted as the minimal system bandwidth. For a gain of 0.01 at low frequency, W_1 is given by:

$$W_1=\frac{(s+513)}{1.42(s+36)}$$

2) Choice of W_2: the most important parameter of W_2 is the cutoff frequency that will limit the maximum system bandwidth to avoid very fast system response. This frequency should be much higher than the system bandwidth.

$$W_2=\frac{(s+100)}{0.1(s+1.10^6)}$$

3) Choice of W_3: as shown in Fig. 7 (b), W_3 is used to filter the external perturbation. Mostly is chosen as low constant and can be adjusted as function of perturbation rejection results.

$$W_3=0.1$$

Based on the filter parameters, the optimal controller K(s) and gamma constant can be found:

$$K(s)=\frac{711.10^3s^3+7.10^{10}.s^2+2.10^{12}s+2.3.10^{12}}{s^4+1.10^5s^3+1.13.109s^2+1.06.10^{12}s+3.10^{12}}$$

$$\gamma=0.996$$

The mathematical result of the controller K(s), shows that the transfers function contains zeros and poles outside the system operation frequency range. The useless zeros and poles can be reduced, but the stability margin thresholds must be always ensured. Reduced second order controller $K_{red}(s)$ is finally obtained:

$$K_{red}(s)=\frac{5.4.10^5s+2.3.10^8}{s2+8.10^3s+1.08.10^7}$$

II. Synthesis of TWUM RST Position Controller

RST controller consists of a discrete time pole placement method based on the resolution of Diophantine equation [17]. As shown in Fig. 8, the RST control is composed by three discrete polynomials ($R(z^{-1})$, $S(z^{-1})$, and $T(z^{-1})$). $B(z^{-1})/A(z^{-1})$ represents the USR60 plant. The eventual perturbations are represented by d. The closed loop transfer function is given by:

$$Y(z^{-1})=\frac{B(z^{-1})T(z^{-1})}{A(z^{-1})S(z^{-1})+B(z^{-1})R(z^{-1})}r(z^{-1})$$

$$+\frac{S(z^{-1})}{A(z^{-1})S(z^{-1})+B(z^{-1})R(z^{-1})}d(z^{-1}) \quad (14)$$

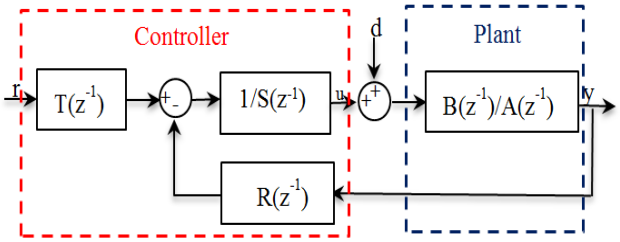

Fig. 8. Discrete-time system controlled by an RST

In (14), the polynomials $T(z^{-1})$ appears only in the numerator giving the supplementary degree of freedom to this controller and can be easily used to ameliorate the tracking performances. The polynomials $R(z^{-1})$ and $S(z^{-1})$ are determined by robust pole placement strategy and will be solution of the Diophantine equation:

$$D(z^{-1})=A(z^{-1})S(z^{-1})+B(z^{-1})R(z^{-1}) \quad (15)$$

The polynomial $D(z^{-1})$ contains the desired poles of the closed loop system and can be written as function of these poles:

$$D(z^{-1})=(1-p_1z^{-1})(1-p_2z^{-2})...(1-p_jz^{-j}) \quad (16)$$

where P_j are the desired poles of closed loop system.

As for the H∞, the desired performance of the closed loop system can be fixed in advance, and then the controller parameters will be determined to achieve these goals. The reference model of the desired closed loop system will be noted H_m:

$$H_m(z^{-1})=\frac{B_m(z^{-1})}{A_m(z^{-1})}=\frac{y(z^{-1})}{r(z^{-1})} \quad (17)$$

To ensure the system stability, the denominator A_m must only contain poles inside the unit circle. The numerator B_m will have as a factor the plant pure delay and the zeros that will be not compensated [17]. Thus, B_m can be written as:

$$B_m(z^{-1})=B^-(z^{-1})B'_m(z^{-1}) \quad (18)$$

In order to obtain unity gain in steady state ($H_m(1)=1$), the polynomial T will be given by [10]:

$$T(z^{-1})=A_0B'_m(z^{-1}) \quad (19)$$

A_0 is a filter polynomial and will be used to ameliorate the tracking performances.

In the case of sinewave reference signal, in order to cancel the steady state error, the auxilliary Diophantine equation must be solved [17]. The auxiliary equation takes into account the angular frequency (ω_0) of the reference signal and can be written as:

$$A_m=(1-2\cos(\omega_0T_s)z^{-1}+z^{-2})L(z^{-1})+B^-B'_m \quad (20)$$

where Ts is the sampling time and $L(z^{-1})$ is a polynomial to be determined.

To deal with the USR60 motor, the continuous time model of is sampled with a sampling period Ts=0.1 ms:

$$G(z^{-1})=\frac{B(z^{-1})}{A(z^{-1})}=\frac{10^{-5}(1.43z^{-2}+1.45z^{-1})}{0.97z^{-2}-1.97z^{-1}+1}$$

The desired performances of the closed loop system are chosen so that the closed loop has a second order type with a damping factor of 0.7 and a bandwidth of 200 rad/s. Thus, a discrete charachteristic polynomial is obtained:

$$A_m=1-1.92z^{-1}+0.932z^{-2}$$

By the resolution of the primary Diophantine Equation (16), the polynomials $S(z^{-1})$ and $R(z^{-1})$ can be obtained:

$$S(z^{-1})=1+0.02z^{-1};\ R(z^{-1})=1.47-1.38z^{-1}$$

For a sinusoidal reference signal with ω_0=10rad/s, the auxiliary Diophantine equation (20) is resolved, and the polynomials $L(z^{-1})$ and $T(z^{-1})$ are found:

$$L(z^{-1})=1+0.034z^{-1}\ ;\ T(z^{-1})=2.46-2.38z^{-1}$$

III. Simulation Results

The proposed control systems of USR60 motor are implemented in MATLAB\Simulink with designed model. The stability, time response, precision, and robustness of the presented methods will be evaluated and compared. The stability margins and the response times of the closed loop system of the two proposed controllers are verified and compared (Fig. 9) giving a time response of 6 ms for the H∞ and 10 ms for the RST. The stability of the closed loop system is guaranteed with the two proposed controllers as indicated in Table I. The phase shift (φ) between the two driven voltages of TWUM must be limited between +/-π/2 for practical use, because outside of this range the motor behavior will be highly nonlinear [13]. This condition will be then taken into account in simulation studies, thus the response times will be slower than those shown in Fig. 9 (b). The time analysis of the closed loop system controlled by H∞ and RST for different position trajectories is shown in Fig. 10. The two proposed controllers show high precision levels with zero steady state error and no overshoot. As mentioned above that the motor parameters will changes as function of operation conditions

(temperature) and driving frequency, the robustness of the position controllers in case of motor parameters variation is also evaluated. For that purposes, the gain and time model constants (K_m, τ) are changed with a ratio of 50% Fig. 11 shows that the control plant is highly robust to the parameters variations with an overshoot less than 1% in case of time constant variation (Fig. 11 (b)). Additional disturbances are also injected to the closed loop system to confirm the perturbation rejection capability of the proposed system. The perturbations are injected respectively to the control signal (φ) and the measured position. The H∞ and RST position controllers show high rejection capability of control signal perturbations as illustrated in Fig. 12 (a). However, when the measured position is perturbed, the H∞ controller has a much better rejection capability as shown in Fig. 12 (b). The later higher performance of H∞ is justified since the weighting filters are sized for such type of perturbations. The load torque has an effect on the precision of TWUM, while it introduces a dead zone on the phase shift-speed characteristic. For that purposes, the performance of the presented position controllers with load torque of 1 N.m is also simulated showing a static error of 0.05% and 0.2% for H∞ and RST, respectively (Fig. 13).

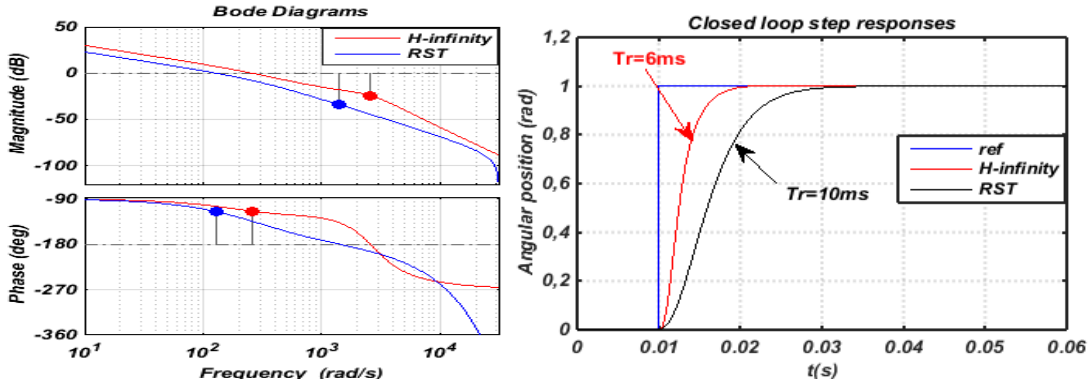

(a) (b)

Fig. 9 (a) Bode diagrams, (b) Step responses

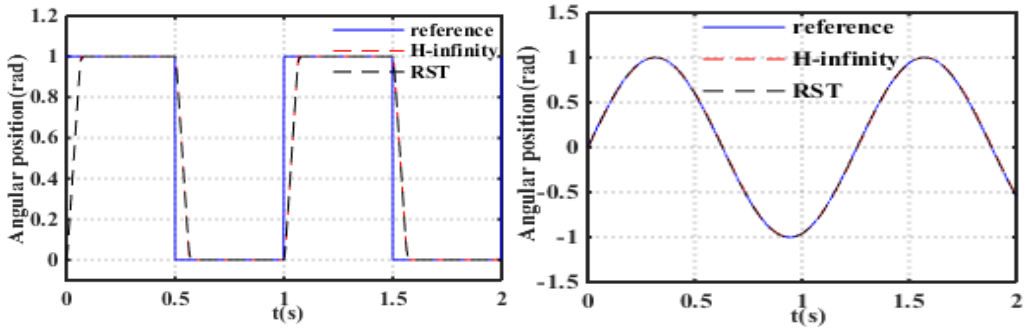

Fig. 10 Comparison of position response

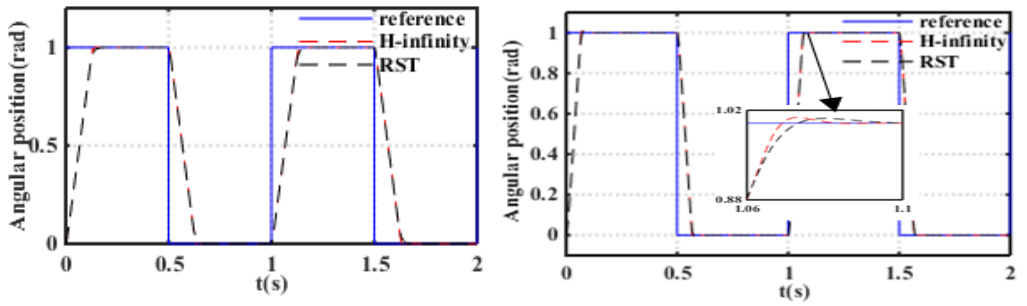

(a) (b)

Fig. 11 Controller performances with modified model parameters: (a) 50% of gain constant, (b) 50% of time constant

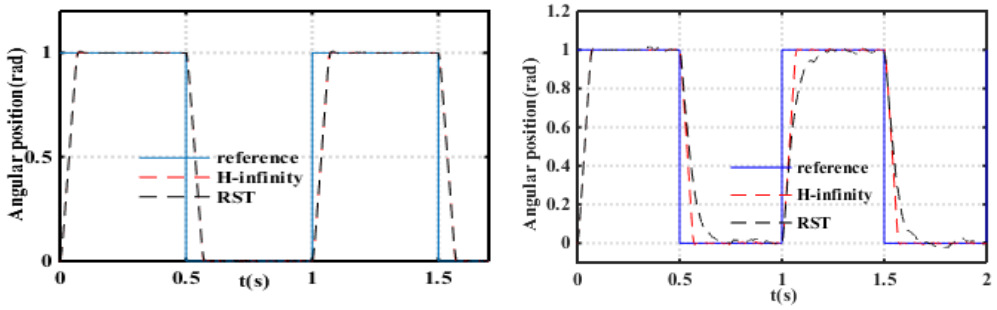

(a) (b)

Fig. 12 Rejection capability of: (a) control signal perturbation, (b) measurement perturbation

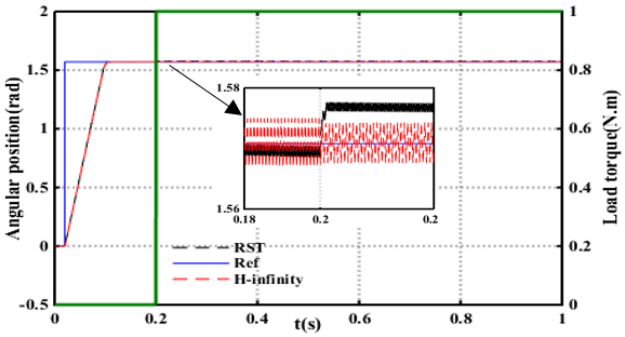

Fig. 13 Load torque effect

TABLE I
CONTROLLER PERFORMANCES

	H-infinity	RST
Phase margin(deg)	70.9	61.5
Gain margin(dB)	24.2	33.4
Response time(ms)	6	10

IV. CONCLUSION

In this paper, Robust H∞ and RST position controllers of rotary TWUM are proposed to deal with high precision positioning system based on TWUM. The requirement of robust controllers for such motors is caused by the motor parameters variation due to the nonlinearity of used piezoelectric materials, operation conditions, and load torque. The H∞ is synthesized in continuous time based on the desired performances of the closed loop system. Weighting filters are used to guarantee the control robustness and system stability. The pole placement RST control is designed in discrete time. The system poles are chosen so that the closed loop system has a second order type with optimal performances.

H∞ and RST position controllers are then simulated with USR60 model that reflect real motor behavior. The stability of the closed loop system and the precision levels without overshoot are satisfied with the two controllers. The robustness of the two controllers in case of motor parameters variation is validated. The proposed system shows also high performances with additional load torque of 1 N.m and in presence of external perturbations with small advantages of the robust H∞ controller.

An experimental test bench is set up for the real time tests of USR60. The next step will be then the experimental validation of the proposed H∞ and RST controllers.

REFERENCES

[1] Sashida, T. Kenjo, " An Introduction to Ultrasonic Motors" Oxford University Press, New York, 1993.
[2] Ch.Zhao," Ultrasonic Motors: Technologies and Applications" Science Press Beijing, 2011.
[3] E.Bekiroglu," Ultrasonic motors: Their models, drives, controls and applications," Journal.of Electroceramics, Vol 20, pp 277-286, August 2008.
[4] A.Gencer, "A new speed/position control technique for travelling wave ultrasonic motor under different load conditions" *PEMC*, Antalya, Sept.2014, pp.65-70
[5] A. Djoewahir, K. Tanaka, S. Nakashima," Adaptive PSO-Based Self-Tuning PID Controller For Ultrasonic Motor," International Journal of Innovative Computing, Information and Control,Vol.9,pp3903-3914,October2013
[6] T. Senjyu, H. Miyazato, S. Yokoda, and K. Uezato, " Position control of ultrasonic motors using neural network," Proceedings of the IEEE International Symposium on Industrial Electronics, ISIE '96, vol. 1, pp. 368-373, 1996.
[7] G.Bal, E. Bekiroglu, S.Demibras, I.Colak, "Fuzzy Logic Based DSP Controlled Servo Position Control for Ultrasonic Motor" Journal of Energy Conversion and Management, Vol.45, 3139-3153 , 2004.
[8] F-J.Lin,R-J.Wai,H-Hai.Yu,"Adaptive fuzzy-neural-network controller for ultrasonic motor drive using LLCC resonant technique. IEEE Transaction on Ultrasonics, Ferroelectrics, and Frequency Control, pp 715-727, 1999.
[9] J.shi, J.Zhao, Z.Cao, Y.Liang, L.Yuan, B.Sun," Self-Tuning Fuzzy Speed Controller of Travelling Wave Ultrasonic Motor," *Int. J. Smart Sensing and intelligent systems*, vol. 7, no. 1, pp.301-320, march.2014
[10] M.Brahim,I.Bahri,Y.Bernard: "Modeling and RST Position Controller of Rotary Traveling Wave Ultrasonic Motor" IEEE Int. Conference on System Process and Control (ICSPC) ;Kuala Lumpur. Malaysia, 2015.
[11] M-Ali Tavallaei, S-Farokh Atashzar, M.Drangova," Robust Motion Control of Ultrasonic Motors Under Temperature Disturbance," *IEEE Trans. Ind. Electron*, vol.63, no.4, pp. 2360-2368, Apr.2016.
[12] M. Budinger, J. -F. Rouchon, B. Nogarede ," Analytical Modeling for the Design of a Piezoelectric Rotating-Mode Motor," *IEEE/ASME Trans. Mechatronics*, vol.9, no.1, March.2015.
[13] T. Senjyu, T. Kashiwagi, K. Uezato," Position control of ultrasonic motors using MRAC and dead-zone compensation with fuzzy inference," IEEE Transaction on Power Electronic, pp 265–272 , 2002.
[14] M.Rakotondrabe; Y.Haddab; Ph.Lutz " Quadrilateral Modelling and Robust Control of a Nonlinear Piezoelectric Cantilever" IEEE Transactions on Control Systems Technology ,Vol.17, pp.528-539, 2009.
[15] J. Doyle, K. Glover, P. P. Khargonekar, and B. A. Francis, "State-space solutions to standard H_2 and H_∞ control problems," *IEEE Trans. Aut. Control*, vol. 34, no. 8, pp. 831–847, Aug. 1989.

[16] H. Ladjal, J-L. Hanus , and A.Ferreira "H_∞ Robustification Control of Existing Piezoelectric-Stack Actuated Nanomanipulators" Int.Conference on Robotics and Automation, pp.3353-3358, 2009.
[17] E.Ostertag, E.Godoy," RST-Controller Design for Sinewave References by Means of an Auxiliary Diophantine Equation ," IEEE Conference on Decision and Control, pp 6905-6910, 2005